Submitted to small
NANO MICRO

DOI: 10.1002/smll.((please add manuscript number))
Article type: Communication

Alignment of Organic Semiconductor Microstripes by Two-Phase Dip-Coating

Mengmeng Li,[†] Cunbin An,[†] Wojciech Pisula,[,†] Klaus Müllen[*,†]*

Mengmeng Li, Cunbin An, Dr. Wojciech Pisula, Prof. Dr. Klaus Müllen
Max Planck Institute for Polymer Research, Ackermannweg 10, 55128 Mainz, Germany
E-mail: pisula@mpip-mainz.mpg.de; muellen@mpip-mainz.mpg.de

Keywords: organic field-effect transistors; surfactant; alignment; ultrathin microstripes; dip-coating

Introduction

Vapor deposition under vacuum is one of the most popular methods for fabrication of the active thin layer of organic field-effect transistors (FETs), but is limited by critical drawbacks including high manufacturing costs and low utilization rate of the semiconductors. In contrast, solution processing is more practical and promising due to its potential in true low-cost mass production of large-area organic electronic devices [1]. Among solution-processing approaches, dip-coating technique has been extensively utilized to control the self-assembly of organic semiconductors which is of vital importance for charge carrier transport. For instance, a monolayer and subsequent aligned nanofibers of poly(2,5-bis(3-alkylthiophen-2-yl)thieno[3,2-b]thiophene) (PBTTT) were precisely deposited by using dip-coating. [2] On the other hand, conjugated small crystalline molecules such as dithieno[2,3-d;2',3'-d']benzo[1,2-b;4,5-b']dithiophene (DTBDT) [3-4], 6,13-bis(triisopropyl-silylethynyl) pentacene (TIPS-pentacene) and 5,11-bis(triethylsilylethynyl) anthradithiophene (FTES-ADT) [5] were dip-coated into monolayer or multilayer microstripes with a high degree of alignment and few grain boundaries leading to superior FET performance. Interestingly, the high sensitivity of such ultrathin stripes makes them promising for applications in gas sensors. [6] However, good solubility of conjugated semiconductors is a prerequisite for solution processing, because a low solubility can result in serious aggregation already in solution

which significantly reduces the homogeneity of resultant films and subsequent device performance. Therefore, a new less solubility-dependent solution method is still in high demand.

There is clear evidence that the growth kinetics of conjugated molecules are strongly dependent on a variety of parameters such as solvent, concentration, temperature and surfactant. [7] Surfactants are common in the field of nanostructure fabrication to change the cohesive energy and determine the competition of crystal facet growth of organic molecules. [7-8] Because of the colloidal stability and/or selective adhesion on certain facets of the surfactant, a high variety of nanoscale objects including cubes, cubooctahedrons, octahedrons [9] and even fullerene-encapsulated rods [10] can be assembled by manipulating the nucleation and the subsequent growth kinetics of conjugated molecules. Nevertheless, it is still a challenge to kinetically tune the assembly of conjugated building blocks into well-ordered, defect-free film structures by solution processing, especially for less soluble molecules. In this communication, we propose a novel solution-processing approach, termed as two-phase dip-coating, to assemble both n- and p-type organic small molecules into highly oriented ultrathin microstripes with the assistance of a surfactant. In this method, an organic semiconductor solution is drop-cast on the surface of an aqueous surfactant solution. Subsequently, dip-coating is carried out, resulting in the alignment of ultrathin microstripes. Three main experimental parameters including aging time of the organic semiconductor solution, pulling speed of the substrate and surfactant concentration in the aqueous solution are investigated, demonstrating significant influences on the self-assembly of the molecules and thus on the formation of microstripes. Moreover, for the n- and p-type conjugated crystalline molecules used in this study, the resultant transistors based on ultrathin aligned microstripes exhibit mobilities for electrons up to 0.12 $cm^2V^{-1}s^{-1}$ and holes of 0.16 $cm^2V^{-1}s^{-1}$, respectively. Such pronounced performance for ultrathin layers confirms that the charge carrier transport of organic semiconductors is primarily attributed to the first few monolayers

near the dielectric. [11] This work demonstrates that two-phase dip-coating is a promising solution-processing approach to deposit and align ultrathin layers of conjugated semiconductors with limited solubility.

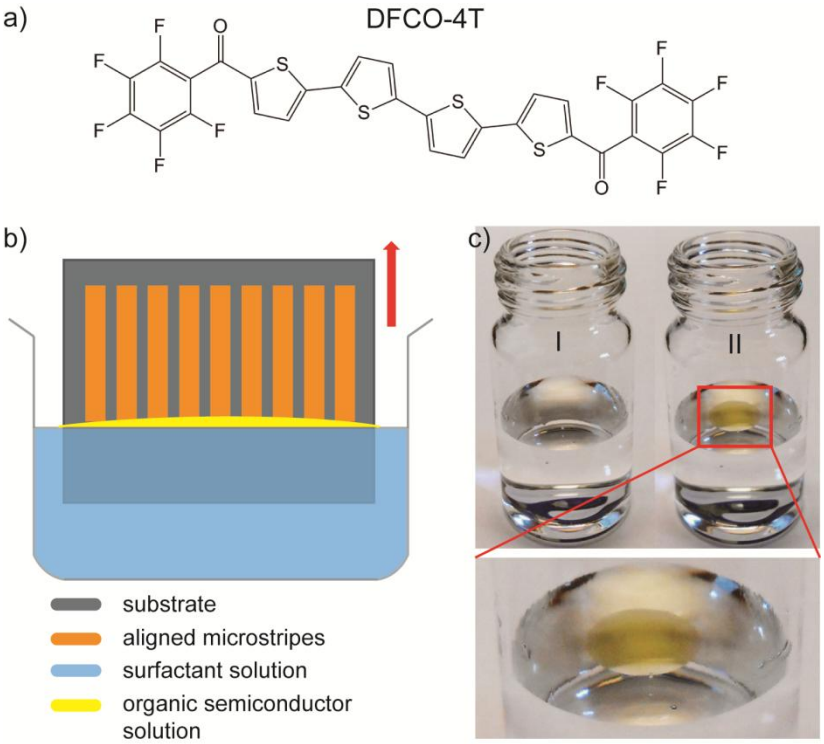

Figure 1. a) Molecular structure of DFCO-4T. b) Schematic illustration of two-phase dip-coating process (red arrow indicates the pulling direction of the substrate). c) Images of the aqueous surfactant solution (I) and two-phase system (II).

Results and discussion

A thiophene-based oligomer, 5,5'''-bis(perfluorophenylcarbonyl)-2,2':5',-2'':5'',2'''-quaterthiophene (DFCO-4T, Figure 1a) is employed in this work as an n-type model compound. Since it is challenging to process DFCO-4T from solution due to its low solubility, in a previous report this molecule was vacuum vapor deposited to films that show an electron mobility up to 0.51 $cm^2V^{-1}s^{-1}$ (Table S1). [12-13] To by-pass the solubility issue, we have developed a new solution-processing approach, named as two-phase dip-coating, by which DFCO-4T ultrathin layers can be grown and aligned in an efficient way. Figure 1b illustrates

schematically the two-phase dip-coating process in which two different liquid phases are used. On top of an aqueous surfactant solution (cetyltrimethylammonium bromide (CTAB) as surfactant at a concentration of 0.01 mg/mL) 40 µL of a chloroform solution of DFCO-4T at the saturated concentration of 0.25 mg/mL is drop-cast. Although chloroform is immiscible with water, and its density (1.48 g/mL) is larger than that of water (1 g/mL), the chloroform solution floats on the surface of the aqueous surfactant solution due to the surface tension of water (Figure 1c). After the chloroform solution has aged for several minutes, ultrathin microstripes can be oriented on a substrate by dip-coating. Herein, the substrates used in all experiments are heavily doped silicon wafers possessing a thermally grown silicon dioxide layer with a thickness of 300 nm.

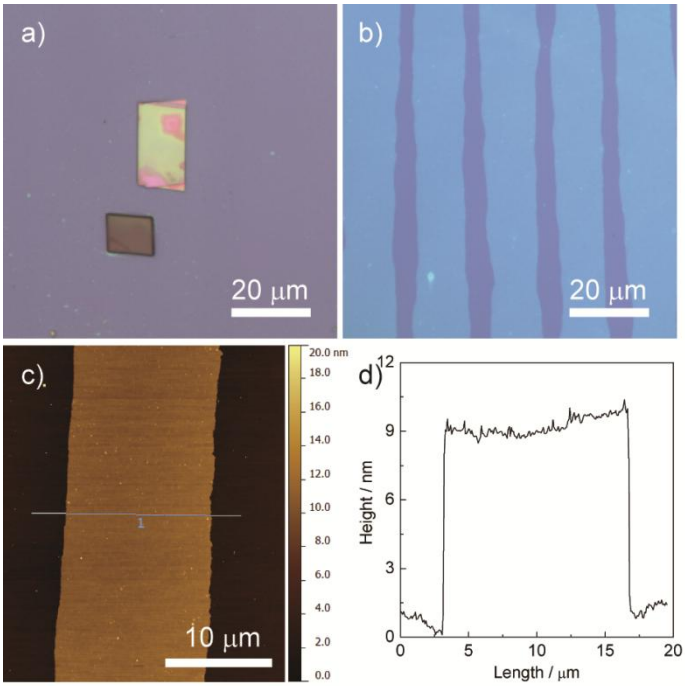

Figure 2. Optical images of DFCO-4T dip-coated from a) chloroform and b) two-phase solution. c) Height AFM image of one single aligned stripe from two-phase dip-coating (line indicates the height plot). d) Height plot for c).

For comparison, DFCO-4T was also dip-coated directly from a chloroform solution, but leading to a random growth of only very few, small crystals on the substrate surface

independent of the casting conditions (Figure 2a). A similar result was observed after spin-coating with an average crystal size of around 10 μm. This undersized microstructure did not allow us to fabricate well operating FET devices. In contrast, ultrathin microstripes with excellent orientation could be obtained by using the two-phase dip-coating. Thereby, the growth axis of the stripes lies along the pulling direction of dip-coating, the width of the microstripes is between 10-20 μm (Figure 2b,c) and the thickness is only about 8 nm as determined from the height section of the atomic force microscopy (AFM) image (Figure 2c,d). In addition to the pronounced alignment of the organic semiconductor, this new dip-coating utilizes much less solvent and material (~40 μL chloroform and ~10 μg DFCO-4T) for each experiment compared to traditional solution deposition.

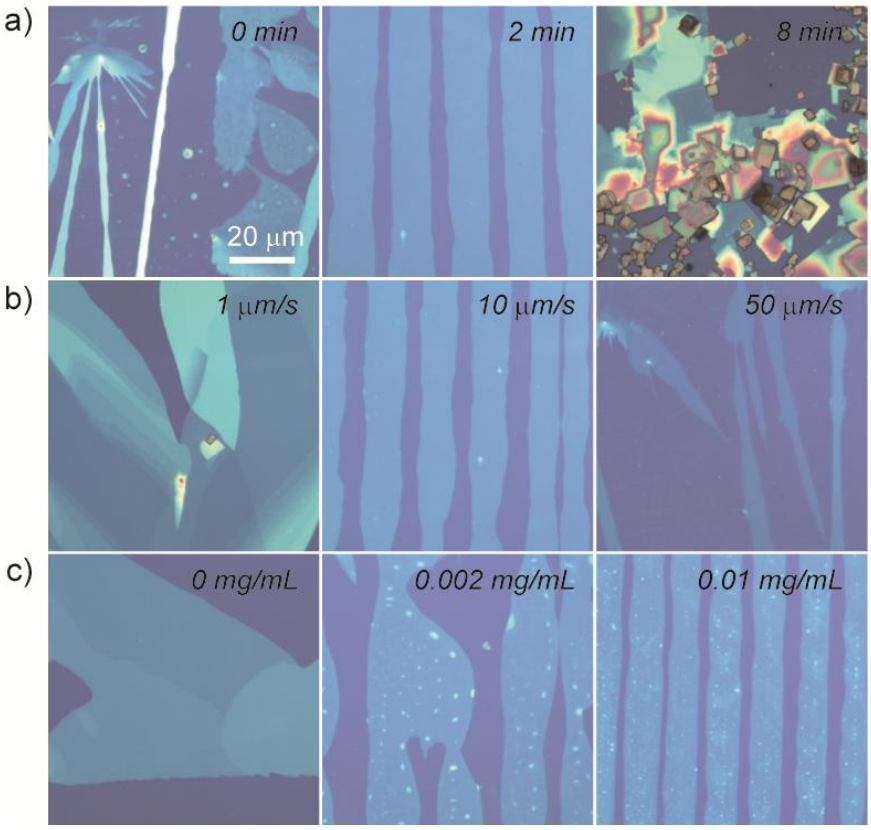

Figure 3. Optical images of dip-coated layers of DFCO-4T from the two-phase system at different conditions. The following parameters are changed: a) aging time of DFCO-4T solution, b) dip-coating speed of substrate, and c) CTAB concentration in aqueous solution.

All images have the same scalebar. The CTAB concentration for a) and b) is 0.01 mg/mL; the aging time for b) and c) is 2 min; the pulling speed for a) and c) is 10 μm/s.

Before alignment by dip-coating from the two-phase system, the floating chloroform droplet needs to be aged on the surface of the CTAB aqueous solution for 2-5 min. This aging time appears to have a significant influence on the microstructure of the microstripes (Figure 3a). When dip-coating is performed immediately after drop-casting of the DFCO-4T solution, that is defined as starting time of the aging (= 0 min), only several irregular structures are grown on the substrate. With extending the time from 2 up to 5 min, the orientation and quality of the microstripes are greatly improved (Figure 3a and S1). A too long aging time (for example 8 min) results in the growth of an irregular film, as shown in Figure 3a.

The dip-coating speed also plays a critical role on the formation of the aligned stripes. In general, the pulling speed determines the film thickness or the amount of material deposited on the substrate. [2] At an aging time of 2 min, more DFCO-4T is deposited with decreasing the dip-coating speed. For low speeds, e.g. 1 μm/s, multilayers and few small crystals are formed on the substrate (Figure 3b). On the contrary, by using a high pulling speed (50 μm/s), much less DFCO-4T is deposited on the substrate surface, leading to the formation of only few irregular stripes with a width of less than 10 μm (Figure 3b). For DFCO-4T the well-aligned microstipes can be obtained by applying the speed of 10 μm/s. The same trend is observed for the aging time of 5 min (Figure S2).

The quality of the aligned microstripes depends sensitively on the surfactant concentration (Figure 3c). An optimum concentration of 0.01 mg/mL CTAB has been identified for the highest degree of alignment of the ultrathin stripes. The orientation is gradually improved with slightly increasing the concentration from 0 mg/mL (without CTAB) starting from a randomly arranged layer. An amount above 0.01 mg/mL CTAB is not applicable because of a

strong hysteresis and decrease in charge carrier mobility of the resulting film. [14] A high CTAB concentration, such as 0.1 mg/mL, largely reduces the orientation and leads to inhomogeneous thin layers (Figure S3).

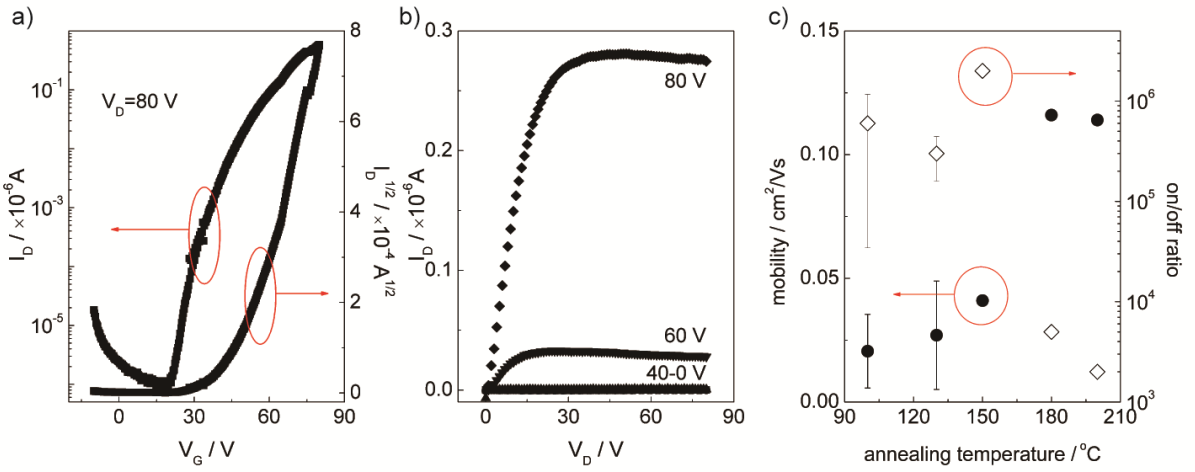

Figure 4. The transfer a) and output b) curves of DFCO-4T FETs based on aligned stripes. The annealing temperature is 130 °C. c) Relation between annealing temperature and electron mobility as well as on/off ratio of aligned DFCO-4T microstripes fabricated by two-phase dip-coating.

To explore the electrical characteristics, the ultrathin aligned microstripes were deposited under optimum conditions which are: aging time of 2 min, pulling speed of 10 μm/s, and CTAB concentration of 0.01 mg/mL. Top-contact bottom-gate (TCBG) FETs were fabricated by evaporating Au source and drain electrodes so that the measurements were performed along the orientation direction. All dip-coating procedures were performed in air, and water was used to form the two-phase system. However, both oxygen and moisture are known to have detrimental effects on the charge carrier transport of organic semiconductors. [15-18] In particular the presence of moisture in the active layer or at the interface with the gate dielectric (especially at the SiO_2 dielectric layer) are important factors responsible for the degradation of the electric performance including decrease in field-effect mobility, current

output, threshold-voltage instabilities, and hysteresis effect. [16-17, 19] The effects of moisture on the charge carrier transport are mainly ascribed to local polarization effects resulting from the large dipole moment of water molecules. [19] Therefore, the microstripes fabricated by two-phase dip-coating were annealed before and after electrode deposition at high temperatures ranging from 100 to 200 ^{o}C, which might remove part of the moisture from the interface and bulk enhancing the field-effect performance. Figure 4a,b exhibits the transfer and output transistors curves of the aligned microstripes after annealing at 130 °C from which an electron mobility of 0.04 $cm^2V^{-1}s^{-1}$ and the on/off ratio of 10^6 are obtained. Compared with previous reports [12-13] the threshold voltage of 60-70 V is significantly improved although still a high value of ~40 V is observed in this study. Trapping at the SiO_2 interface and contact resistance of the electrodes can be responsible for such high threshold voltages. [20-21] In addition, a relation between electron transport and annealing temperature is found (Figure 4c). With increasing the annealing temperature from 100 to 150 ^{o}C, the electron mobility is doubled from 0.02 to 0.04 $cm^2V^{-1}s^{-1}$, while at 180 ^{o}C the value jumps to 0.12 $cm^2V^{-1}s^{-1}$. Above this temperature, the mobility remains almost unchanged. The ultrathin stripes cannot be annealed above 250 °C that is close to the sublimation temperature of DFCO-4T [13] leading to the evaporation of the material from the surface. On the other hand, at high annealing temperatures (180-200 ^{o}C) the on/off ratio of the transistors decreases from around 10^6 to 10^3-10^4 due to the increase in off-current.

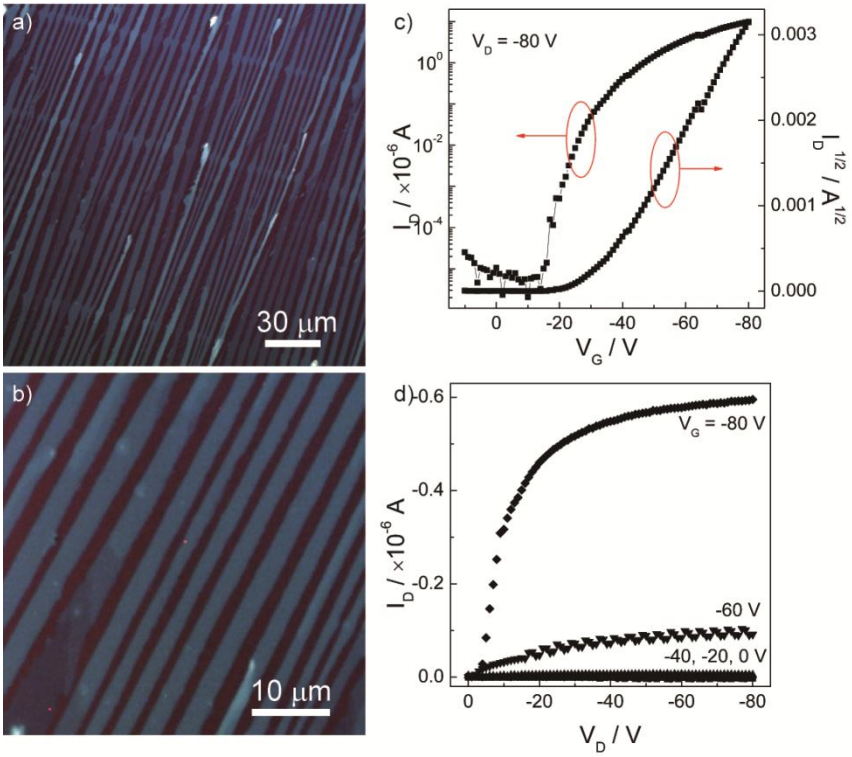

Figure 5. a,b) Optical images of DTBDT aligned microstripes by two-phase dip-coating. The transfer c) and output d) curves of corresponding FETs.

Besides DFCO-4T, this two-phase dip-coating method is also applicable to other conjugated crystalline molecules such as DTBDT (Figure S4). Figures 5a,b show the microstructure of DTBDT microstripes aligned by two-phase dip-coating. The width of only 5 μm for a single stripe is smaller than that of DFCO-4T, but the length is up to 1-2 cm. From the height plot of the AFM image (Figure S5) a thickness of around 12 nm is determined. Since the height of a DTBDT monolayer is ~2 nm [3-4], these microstripes should be composed of approximately 6 layers. An annealing procedure at 115 ^{o}C before and after electrode deposition is also carried out to enhance the charge carrier transport. The transfer and output plots in Figures 5c,d indicate a good field-effect behavior for the DTBDT microstripes with the hole mobility of 0.16 $cm^2V^{-1}s^{-1}$ and the on/off ratio of 10^6, which are in a similar range as previously reported values [3-4]. Very recently Li et al has reported DTBDT ultrathin microstripes with

around 10 μm in width and with a mobility of 0.1-0.2 $cm^2V^{-1}s^{-1}$. [4b] This mobility value is similar to our results (0.16 $cm^2V^{-1}s^{-1}$), but it has to be noted that the width of our microstripes is 5 μm, only half as much as the value in Ref. 4b. This comparison indicats that narrower stripes do not lead to an enhanced charge transport and the potential effect of confinement within this size range is neglected. In comparison to the branched microstripes obtained by direct dip-coating [4], the well-aligned parallel stripes fabricated by the two-phase method might be more beneficial for the deposition of the gold electrodes on the better defined, active film. In order to study the molecular organization in the aligned stripes, grazing incidence wide-angle X-ray scattering (GIWAXS) measurement was carried out. However, because of the extremely small scattering volume of the ultrathin films only very few scattering reflections were obtained which are not sufficient for a comprehensive analysis of the organization.

Molecular self-assembly from solution results from a complicated combination of molecule-molecule, molecule-solvent and molecule-substrate interactions. [22] The self-assembly mechanism of the ultrathin aligned stripes by two-phase dip-coating is described as follows. During the aging process of the chloroform solution on top of the water surface, the organic semiconductor is recrystallized to form crystal nuclei at the interface of both liquids because of the presence of water as bad solvent for the molecules. At the same time, a certain amount of CTAB can diffuse from water into the chloroform solution, which is supposed to change the cohesive energy of conjugated molecules, determine their crystal facet growth and subsequently induce molecular crystallization on the substrate. The surfactant exhibits a crucial role for the crystal shape, as shown by the two experiments in Figures 2a and S6. [7] Direct dip-coating from DFCO-4T chloroform solution with 0.1 mg/mL CTAB causes the formation of diamond-shaped crystals, in comparison to rectangular ones without surfactant. On the basis of these recrystallized crystal nuclei, well-aligned microstripes are grown on the

substrate along the pulling direction with the assistance of CTAB. In this study, both conjugated crystalline molecules can be hardly deposited on the substrate by direct dip-coating from chloroform solution. As a result, the deposition of microstripes could also benefit from additional repelling forces caused by the immiscibility of chloroform and water in the two-phase dip-coating.

Conclusion

Alignment of microstripes is successfully realized by two-phase dip-coating, especially for conjugated semiconductors with low solubility. This method is based on the application of a surfactant as an assistant agent and a phase-separated binary liquid mixture. The aging time, dip-coating speed, and surfactant concentration play an essential role on the self-assembly of ultrathin aligned stripes. By using this approach, both n- and p-type small molecules can be assembled into aligned microstripes that show good field-effect behavior in devices with highest charge carrier mobilities of 0.12 $cm^2V^{-1}s^{-1}$ for electrons of DFCO-4T and 0.16 $cm^2V^{-1}s^{-1}$ for holes of DTBDT. Since these microstripes have a thickness of only 8-12 nm (4-6 layers), their outstanding capability of charge carrier transport provides further evidence that only the first few semiconducting monolayers near the dielectric interface are mainly responsible for the charge carrier transport. [11]

The dip-coating process has been commercially utilized for the deposition of thin films such as sol-gel and antireflection layers since the mid of last century. [23-24] In many cases, factors such as good solubility are limiting the further development of dip-coating for practical applications of organic electronics. We believe that the two-phase dip-coating approach can open a new pathway for alignment of conjugated small crystalline molecules by solution-processing independent of molecular solubility. Since this method is applicable for both n- and p-type organic semiconductors, our future work will focus on the alignment of

ambipolar composite ultrathin microstripes, facilitating the fabrication of complementary circuits.

Experimental Section

Two-phase dip-coating approach. DFCO-4T was purchased from Polyera Corporation (ActivInk^{TM} N0400). The saturated solution of DFCO-4T was prepared using chloroform as solvent. The surfactant, cetyltrimethylammonium bromide (CTAB, Alfa), was dissolved in ultrapure water (Milli-Q). Heavily doped silicon wafers with a thermally grown silicon dioxide layer with the thickness of 300 nm were used as substrates. The wafers were firstly cleaned via ultrasonication in acetone for 10 min, following via sonication in isoproponal for 10 min. 10 mL CTAB solution was injected into a 20 mL glass bottle as base liquid. Then a droplet (~40 μL) of DFCO-4T solution was dropped onto the surface of surfactant solution. After this two-phase system was aged for a few minutes, the dip-coating was processed by using cleaned substrate. The synthesis of DTBDT is described elsewhere, [3] and its two-phase dip-coating procedure is analogous to that of DFCO-4T.

Characterizations. The optical images were taken by a digital camara (Nikon) and a Zeiss Axiophoto microscope equipped with a Hitachi KP-D50 color digita CCD camera. A Digital Instruments Nanoscope IIIa Atomic Force Microscopy (AFM) in tapping mode was utilized to record AFM images.

Device Fabrication and Measurements. We fabricated top-contact bottom-gate FETs. The source and drain electrodes with 80 nm in thickness and 25 μm in channel length were deposited by Au evaporation. A Keithley 4200-SCS was used for all standard electrical measurements in a glovebox under nitrogen atmosphere.

Supporting Information

Supporting Information is available online from the Wiley Online Library or from the author.

Acknowledgements
M. L. thanks Prof. Dr. Martin Baumgarten for his useful suggestions and acknowledges financial support from the ERC Advanced Grant NANOGRAPH (AdG-2010-267160).

1. Gather, M. C.; Köhnen, A.; Meerholz, K., *Advanced Materials* **2011,** *23* (2), 233-248. DOI 10.1002/adma.201002636.
2. Wang, S.; Kiersnowski, A.; Pisula, W.; Müllen, K., *Journal of the American Chemical Society* **2012,** *134* (9), 4015-4018. DOI 10.1021/ja211630w.
3. Gao, P.; Beckmann, D.; Tsao, H. N.; Feng, X.; Enkelmann, V.; Baumgarten, M.; Pisula, W.; Müllen, K., *Advanced Materials* **2009,** *21* (2), 213-216. DOI 10.1002/adma.200802031.
4. a) Li, L.; Gao, P.; Schuermann, K. C.; Ostendorp, S.; Wang, W.; Du, C.; Lei, Y.; Fuchs, H.; Cola, L. D.; Müllen, K.; Chi, L., *Journal of the American Chemical Society* **2010,** *132* (26), 8807-8809. DOI 10.1021/ja1017267; b) Li, L.; Gao, P.; Wang, W.; Müllen, K.; Fuchs, H.; Chi, L., *Angewandte Chemie International Edition* **2013**, *52*, 12530-12535. DOI 10.1002/anie.201306953.
5. Jang, J.; Nam, S.; Im, K.; Hur, J.; Cha, S. N.; Kim, J.; Son, H. B.; Suh, H.; Loth, M. A.; Anthony, J. E.; Park, J.-J.; Park, C. E.; Kim, J. M.; Kim, K., *Advanced Functional Materials* **2012,** *22* (5), 1005-1014. DOI 10.1002/adfm.201102284.
6. Li, L.; Gao, P.; Baumgarten, M.; Müllen, K.; Lu, N.; Fuchs, H.; Chi, L., *Advanced Materials* **2013**, n/a-n/a. DOI 10.1002/adma.201301138.
7. Lin, Z.-Q.; Sun, P.-J.; Tay, Y.-Y.; Liang, J.; Liu, Y.; Shi, N.-E.; Xie, L.-H.; Yi, M.-D.; Qian, Y.; Fan, Q.-L.; Zhang, H.; Hng, H. H.; Ma, J.; Zhang, Q.; Huang, W., *Acs Nano* **2012,** *6* (6), 5309-5319. DOI 10.1021/nn3011398.
8. Hollingsworth, M. D., *Science* **2002,** *295* (5564), 2410-2413. DOI 10.1126/science.1070967.
9. Kang, L.; Fu, H.; Cao, X.; Shi, Q.; Yao, J., *Journal of the American Chemical Society* **2011,** *133* (6), 1895-1901. DOI 10.1021/ja108730u.
10. Sandanayaka, A. S. D.; Murakami, T.; Hasobe, T., *The Journal of Physical Chemistry C* **2009,** *113* (42), 18369-18378. DOI 10.1021/jp9063577.
11. Dinelli, F.; Murgia, M.; Levy, P.; Cavallini, M.; Biscarini, F.; de Leeuw, D. M., *Physical Review Letters* **2004,** *92* (11), 116802.
12. Letizia, J. A.; Cronin, S.; Ortiz, R. P.; Facchetti, A.; Ratner, M. A.; Marks, T. J., *Chemistry – A European Journal* **2010,** *16* (6), 1911-1928. DOI 10.1002/chem.200901513.
13. Letizia, J. A.; Facchetti, A.; Stern, C. L.; Ratner, M. A.; Marks, T. J., *Journal of the American Chemical Society* **2005,** *127* (39), 13476-13477. DOI 10.1021/ja054276o.
14. Shih, C.-J.; Paulus, G. L. C.; Wang, Q. H.; Jin, Z.; Blankschtein, D.; Strano, M. S., *Langmuir* **2012,** *28* (22), 8579-8586. DOI 10.1021/la3008816.
15. Aguirre, C. M.; Levesque, P. L.; Paillet, M.; Lapointe, F.; St-Antoine, B. C.; Desjardins, P.; Martel, R., *Advanced Materials* **2009,** *21* (30), 3087-3091. DOI 10.1002/adma.200900550.
16. Li, D.; Borkent, E.-J.; Nortrup, R.; Moon, H.; Katz, H.; Bao, Z., *Applied Physics Letters* **2005,** *86* (4), 042105-3.
17. Hoshino, S.; Yoshida, M.; Uemura, S.; Kodzasa, T.; Takada, N.; Kamata, T.; Yase, K., *J Appl Phys* **2004,** *95* (9), 5088-5093.
18. Kim, W.; Javey, A.; Vermesh, O.; Wang, Q.; Li, Y.; Dai, H., *Nano Lett* **2003,** *3* (2), 193-198. DOI 10.1021/nl0259232.

19. Sirringhaus, H., *Advanced Materials* **2009,** *21* (38-39), 3859-3873. DOI 10.1002/adma.200901136.
20. Chua, L.-L.; Zaumseil, J.; Chang, J.-F.; Ou, E. C. W.; Ho, P. K. H.; Sirringhaus, H.; Friend, R. H., *Nature* **2005,** *434* (7030), 194-199. DOI 10.1038/nature03376.
21. Katz, H. E.; Hong, X. M.; Dodabalapur, A.; Sarpeshkar, R., *J Appl Phys* **2002,** *91* (3), 1572-1576.
22. Palermo, V.; Samorì, P., *Angewandte Chemie International Edition* **2007,** *46* (24), 4428-4432. DOI 10.1002/anie.200700416.
23. Yimsiri, P.; Mackley, M. R., *Chemical Engineering Science* **2006,** *61* (11), 3496-3505. DOI 10.1016/j.ces.2005.12.018.
24. Puetz, J.; Aegerter, M. A., Dip Coating Technique. In *Sol-Gel Technologies for Glass Producers and Users*, Aegerter, M.; Mennig, M., Eds. Springer US: 2004; pp 37-48.

Submitted to small

The table of contents

A new solution-processing method, termed as two-phase dip-coating, is proposed for the alignment of organic semiconductors, with the assistance of a surfactant. The resultant ultrathin aligned microstripes for both n- and p-type conjugated molecules show an electron mobility of 0.12 $cm^2V^{-1}s^{-1}$ and a hole mobility of 0.16 $cm^2V^{-1}s^{-1}$, respectively.

Keyword

organic field-effect transistors; surfactant; alignment; ultrathin microstripes; dip-coating

Authors

Mengmeng Li,[†] Cunbin An,[†] Wojciech Pisula,[,†] Klaus Müllen[*,†]*

Title

Alignment of Organic Semiconductor Microstripes by Two-Phase Dip-Coating

ToC figure

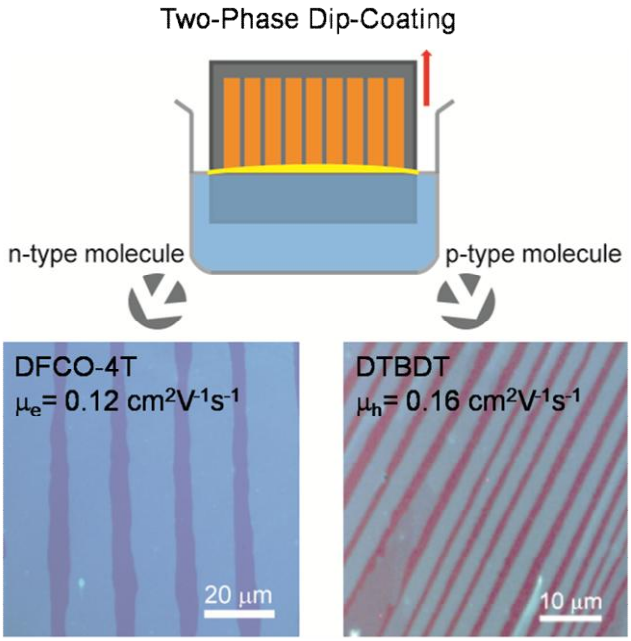

Submitted to small

Supporting Information

for *Small*, DOI: 10.1002/smll.((please add manuscript number))

Alignment of Organic Semiconductor Microstripes by Two-Phase Dip-Coating

Mengmeng Li,[†] Cunbin An,[†] Wojciech Pisula,[,†] Klaus Müllen[*,†]*

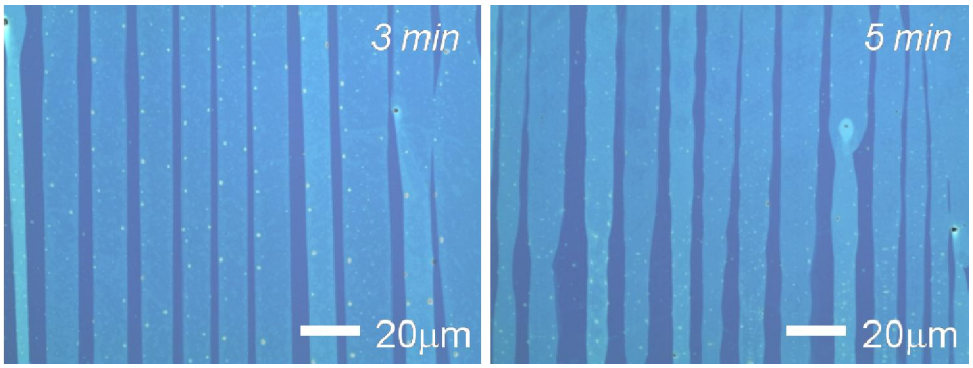

Figure S1. Aligned DFCO-4T microstripe arrays fabricated after aging times of 3 and 5 min. The dip-coating speed is 10 μm/s and the CTAB concentration is 0.01 mg/mL.

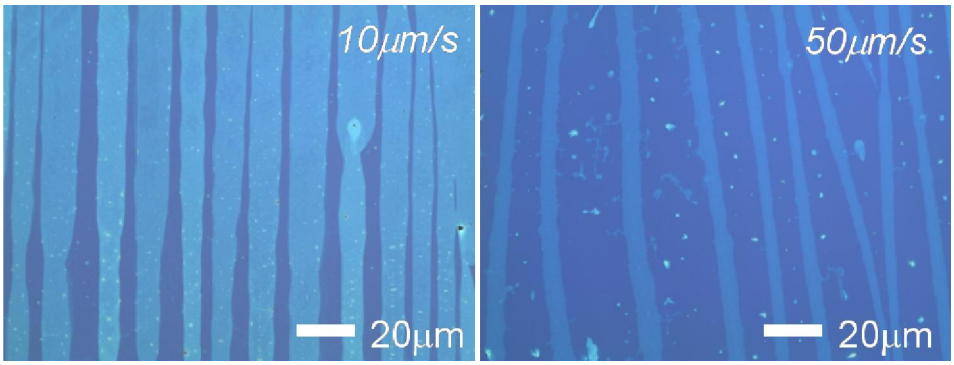

Figure S2. The influence of dip-coating speed on the formation of aligned DFCO-4T microstripes. The aging time is 5 min and the CTAB concentration is 0.01 mg/mL.

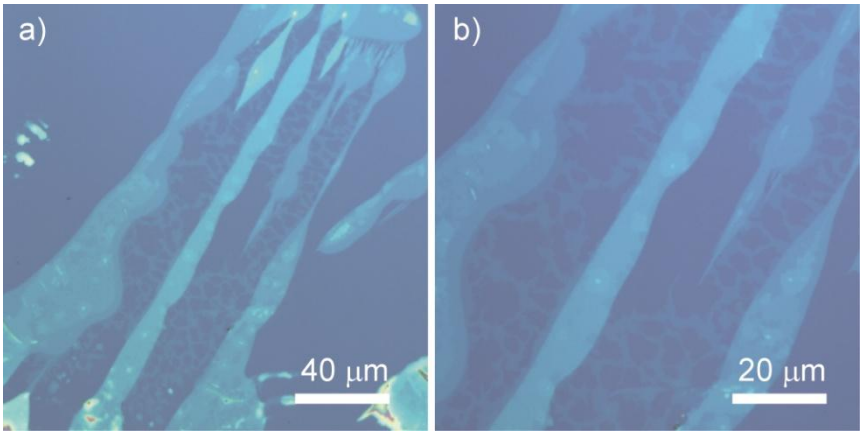

Figure S3. The influence of high CTAB concentration (0.1 mg/mL) on the morphologies of DFCO-4T microsturctures by two-phase dip-coating. The aging time is 2 min and the pulling speed is 10 μm/s.

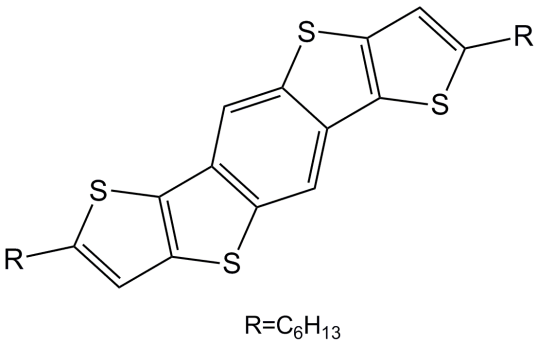

Figure S4. Molecular structure of DTBDT.

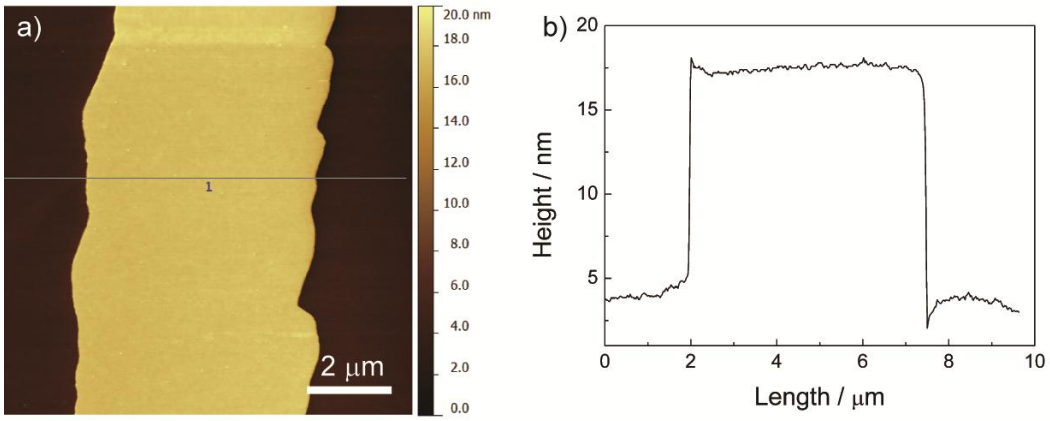

Figure S5. a) Height AFM image of one single DTBDT aligned stripe by two-phase dip-coating (line indicates the height plot). b) Height plot for a).

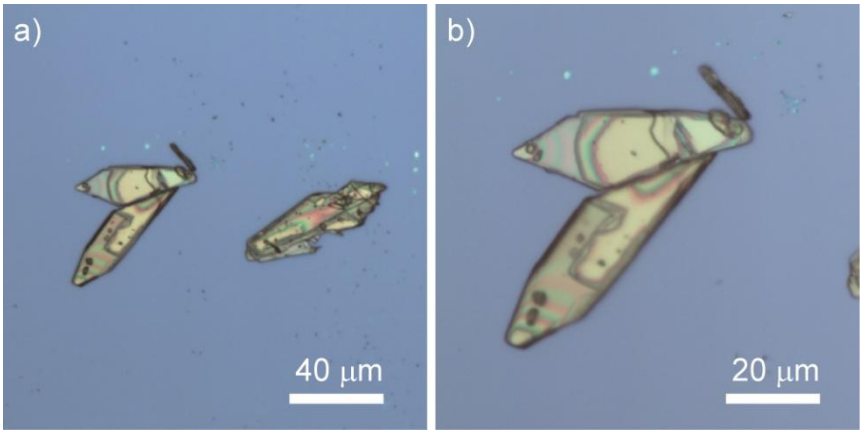

Figure S6. The optical images of DFCO-4T crystals by directly dip-coating from chloroform solution with 0.1 mg/mL CTAB. The pulling speed of the substrate is 10 μm/s.

Table S1. Comparison of the experimental details and transistor performance between two-phase dip-coating and Ref. 13.

	Results in Ref. 13		Our results
Deposition methods	Vacuum vapor deposition	Drop-casting	Two-phase dip-coating
Substrate deposition temperature	80 °C	120 °C	Room temperature
Surface modification	HMDS-treated	HMDS-treated	Bare
Film thickness	50 nm	Order of μm	8 nm
Electron mobility	0.45-0.51 $cm^2V^{-1}s^{-1}$	0.21 $cm^2V^{-1}s^{-1}$	0.12 $cm^2V^{-1}s^{-1}$